Fourth International Conference on Generation IV & Small Reactors (G4SR-4)
Toronto, ON, Canada, October 3 – October 6, 2022

GAS-TUNGSTEN ARC WELDABILITY OF INCOLOY 800H WITH INCONEL 625 FILLER MATERIAL IN THE APPLICATION OF HTGRS

L. Xiao and W. Li

Canadian Nuclear Laboratories, Chalk River, Ontario, Canada

Lin.Xiao@cnl.ca, Wenjing.Li@cnl.ca

Abstract

Incoloy 800H is a potential core component material for high temperature gas-cooled reactors (HTGRs), with expected operating temperatures above 750 °C. However, creep rupture resistance of conventional Incoloy 800H welds is significantly degraded when the environmental temperature is higher than 475 °C. The objective of this work is to explore the weldability of Incoloy 800H using the gas tungsten arc welding (GTAW) technique with Inconel 625 filler material. Welding microstructure was characterized using optical microscopy, scanning electron microscopy, and transmission electron microscopy. Micro-hardness and high temperature tensile properties (conducted at 760 °C) of Incoloy 800H welds were measured. Incoloy 800H welded with Inconel 625 filler material showed superior high temperature tensile strength compared to the unwelded base metal (BM). The weld failure occurred outside the welding zones. The Incoloy 800H welds showed more than a 50% increase in yield strength compared to the BM. In contrast, the ultimate tensile strength is minimally affected by welding. Microstructural characterization shows that the welding process induced the diffusion of alloying elements across fusion boundaries and the formation of a large number of nano-precipitates in the heat-affected zone and fusion zone. As a result, the high temperature mechanical properties of Incoloy 800H were enhanced due to the effects of solid solution strengthening and precipitation strengthening.

1. Introduction

Although renewable energy sources offer the possibility of clean energy, there are concerns about their economic efficiency and reliability, whereas the economic reliability of nuclear energy has been demonstrated by the reactors operating today. Nuclear energy is regarded as one of most efficient and clean (low-carbon) energy sources to combat the effects of climate change [1]. Rather than relying on current-generation-reactors, an international collaboration is directed toward the development of next-generation (i.e., Generation IV) reactors that will produce abundant, safe and reliable energy using proliferation-resistant fuel technologies [2]. The high temperature gas-cooled reactor (HTGR), which is one of the most promising nuclear systems among the Generation-IV (Gen IV) reactors, provides more efficient electricity generation and a significant safety advantage compared with conventional light water reactors (LWRs) during postulated loss of coolant accidents (LOCA). Incoloy 800H has long been used as a construction material in high-temperature, extreme oxidation and corrosive environments. Its desirable mechanical and corrosion properties and satisfactory service history have prompted this alloy to be selected as a potential material for use as nuclear fuel cladding, pressure vessel, and heat exchanger materials for HTGRs [3,4]. An excellent combination of strength and ductility was achieved in the

Incoloy 800H weldments with the Inconel 82 filler material (Ni+Co 67.0% min, Cr 18.0-22.0, Si 0.50 max, Ti 0.75 max, Nb+Ta 2.0-3.0, C 0.10 max, Mn 2.5-3.5, Fe, 3.0 max, Cu, 0.50 max) at both room temperature and elevated temperatures [3-6]. However, creep rupture resistance is significantly degraded when the environmental temperature is higher than 475 °C [3-6]. Therefore, a suitable alternative filler material is vital to maintain stable mechanical and corrosion properties of Incoloy 800H in reactor core components up to 760 °C, as required for HTGR applications.

Although filler materials are not specifically designed for nuclear application, they should have a low radioactivity after neutron irradiation. The filler material chemical composition should match with the major elements in the base metal (BM). They should have stable mechanical and corrosion properties. High-temperature creep resistance and fatigue strength of filler materials should be comparable to that of the BM when applied in long-term high temperature service environments. Inconel 625 is selected as a filler material due to its high strength and excellent corrosion resistance at high temperature and outstanding creep resistance over 593 °C. The objective of this work is to characterize the weldability and mechanical properties of Incoloy 800H using the filler material comprised of Inconel 625.

2. Material and Experimental Procedure

2.1 Material

Incoloy 800H plates: 508 mm (20″) in length, 152 mm (6″) in width and 19 mm (3/4″) in thickness, which were melted and manufactured by VDM Metals, Germany, were purchased from American Special Metals Corporation. The Inconel 625 filler wires with a diameter of 1.6 mm (0.0625”) were purchased from Haynes International. Table 1 shows the chemical compositions of the Incoloy 800H plates and Inconel 625 filler wires.

Table 1: Chemical Composition of the Incoloy 800H Plates and Inconel 625 Filler Wires

Alloys	Fe	Ni	Cr	Mo	Nb	Mn	C	Si	Al	Ti	Co
Incoloy 800H	45.5	30.8	20.8	/	/	0.7	0.08	0.4	0.49	0.52	/
Inconel 625	<5.0	>58.0	20.0~ 23.0	8.0~ 10.0	3.15~ 4.15	<0.5	<0.1	<0.5	<0.4	<0.4	<1.0

2.2 Welding Procedure

A double-sided U-type notch butt joint was designed. A U-type bottom with a notch of 6 mm in width was adopted to increase the flowability of molten liquid in the fusion zone (FZ). The straight side surface of the U-groove was utilized for mechanical property testing to reduce the variation of the weld metal (WM)/filler materials within the gage length of the samples.

Gas tungsten arc welding (GTAW) was used to fabricate the Incoloy 800H weldments. A direct current (DC) of 230 amps was used. A multi-pass welding technique with a low welding speed was adopted to prevent the formation of cracking in the weldments. Welding was started from the “U-type” notch side, and then flipped to weld the back. The plates were flipped back and forth after each pass. An average of fifteen passes were conducted to complete a plate of weldment. Argon was used to protect the weld from oxidizing. The argon flow gauge was set at 20 psi. Neither

post-weld heat treatment nor post-weld rolling was applied since the distortion of weldment was minor after welding.

2.3 Microstructural Characterization and Mechanical Property Measurement

Rod "dog-bone" tension specimens of 6.4 mm in diameter and 50.8 mm in gauge length were machined from the welded plates parallel to the rolling direction and perpendicular to weld seam. A uniform cylindrical welding zone of 6.4 mm in diameter and approximately 6 mm in length was located in the middle of gauge length of the mechanical testing samples. Transverse sections of the weld seams were prepared for metallographic analysis. Sectioned weld samples were mounted in epoxy. Specimens were ground and polished, using silicon carbide paper and alumina powder, respectively, and then etched. Microstructural characterization of welds was performed using an optical microscope (OM), field emission scanning electron microscope (SEM) with energy dispersive X-ray spectrometer (EDS), and transmission electron microscope (TEM).

Micro-hardness testing with a diamond indenter was performed on each specimen prepared for metallographic imaging. An indention load of 0.3 kgf was used. High temperature tension tests were performed to assess mechanical properties of the welds. Tensile tests were conducted using an MTS testing system. A high-temperature Epsilon extensometer with a gauge length of 50 mm was used to measure the displacement of the sample. A low tensile strain rate of 1×10^{-4} s^{-1} was used since Incoloy 800H has a high plastic strain rate sensitivity. After reaching the specimens' test temperature of 760 °C, this temperature was maintained for 30 minutes to achieve thermal equilibrium between the sample, the grips, and the pulling rods, after which the specimens were pulled to failure.

3. Results and Discussion

3.1 Microstructure of Base Metal and Welds

Fig. 1(a) shows optical microstructure of the Incoloy 800H base metal (BM) at the as-received condition in the ND-TD (normal direction-transverse direction) plane. The Incoloy 800H has an average grain size of 180 μm. The Incoloy 800H BM shows equiaxed grains of a single austenitic phase with many annealing twins, as indicated by empty arrows in Fig. 1(a). Some particles are dispersed in the grain matrix and particularly at grain boundaries. Fig. 1(b) shows the SEM photomicrograph of the as-received BM, as well as the EDS spectra taken from different sample locations. EDS analysis shows that the predominant particles are Ti(C,N) in the Incoloy 800H BM, as shown in Fig. 1(c) and (d).

The typical microstructure across welding zones is shown in Fig. 2. A macroscopic view of the weld seam cross-section is shown in Fig. 2(a). The weld seam appears sound with no indication of large pores or hot cracking. Fig. 2(b) shows microstructure formed in the fusion zone (FZ). The weld FZ is comprised of an equiaxed dendritic structure. Epitaxial cellular solidification was observed to grow from the Incoloy 800H substrate into the FZs of the weld, as indicated by the arrow in Fig. 2(c). Areas of equiaxed grains were observed in the heat-affected zone (HAZ) and BM, as shown in Fig. 2(c). No obvious grain size changes are visible in the HAZ.

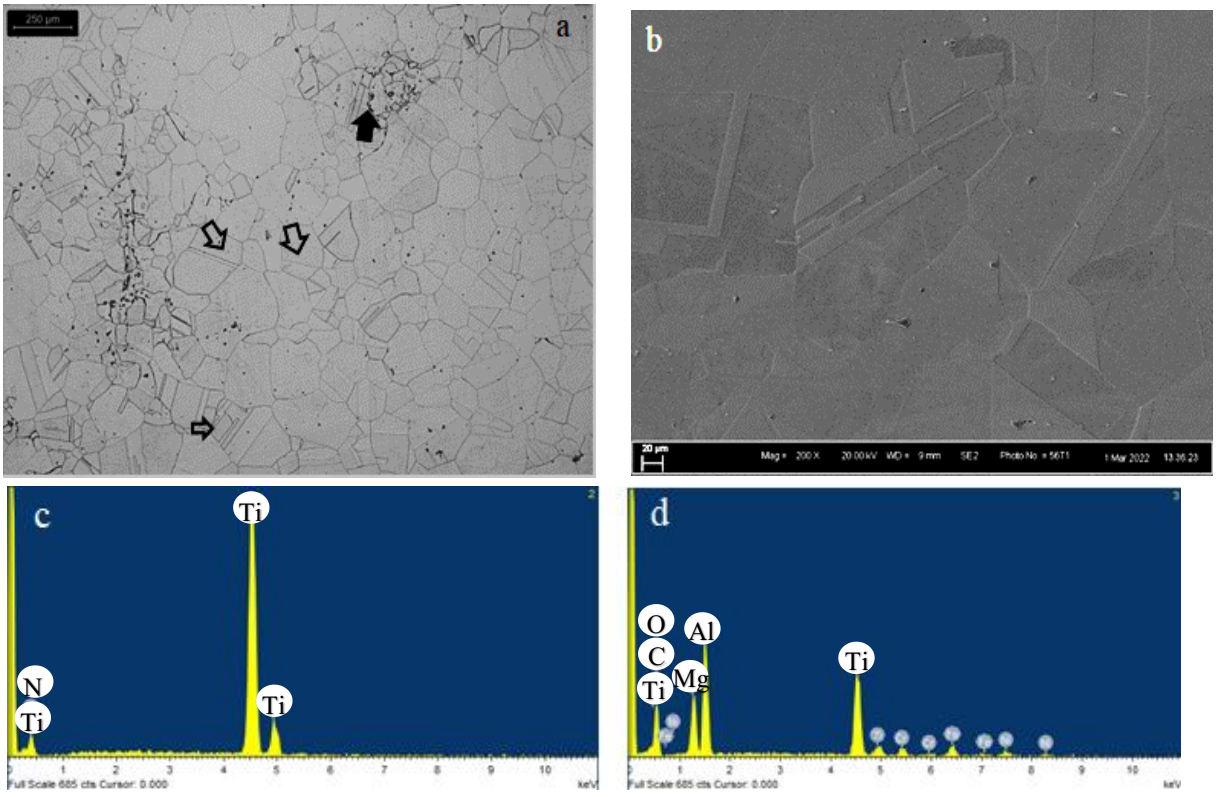

Figure 1: Typical Microstructure of Incoloy 800H BM in As-received Condition, (a) Optical Image, (b) SEM Image, (c) and (d) EDS Analysis of Ti(N,C) Precipitates

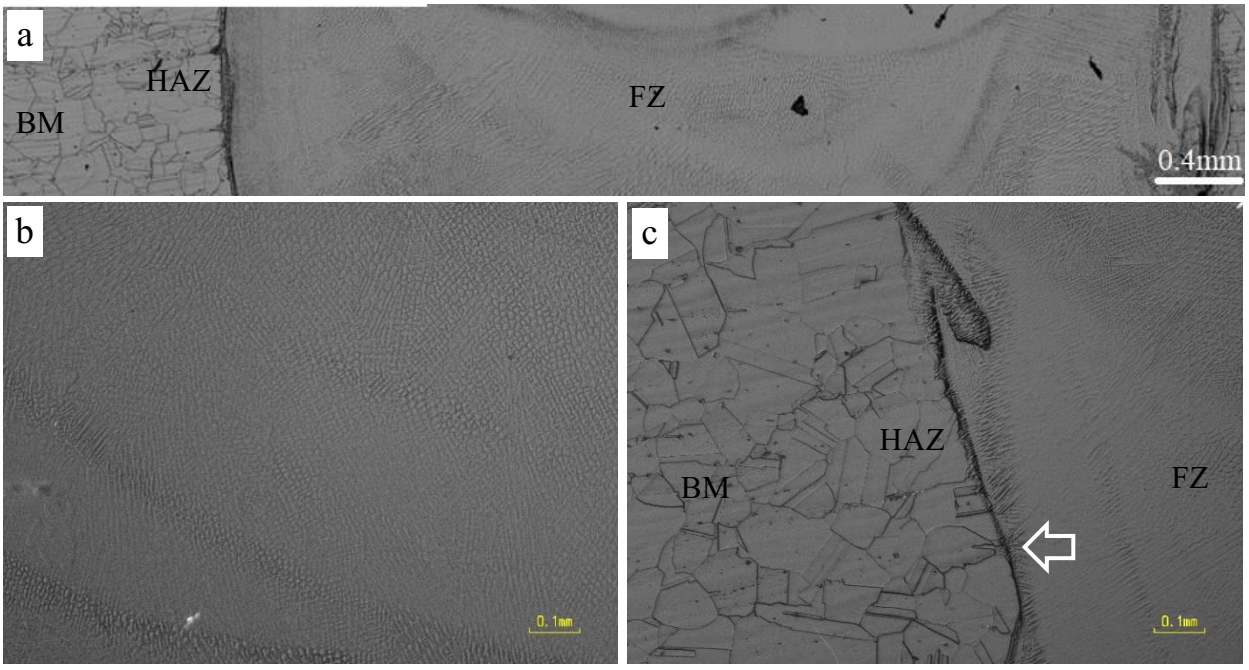

Figure 2: Typical Optical Microstructures across Weld of Incoloy 800H. (a) Macroscopic Welding Zones, (b) FZ, (c) Interface between HAZ and FZ

3.2 Micro-Hardness and High Temperature Tensile Mechanical Properties

For welds with nonhomogeneous microstructures, micro-hardness testing can probe and compare the strength of specific regions of welds. Fig. 3 shows the micro-hardness distribution across welding zones of Incoloy 800H. Four vertical dashed lines approximately indicate the locations of BM/HAZ and HAZ/FZ boundaries. The micro-hardness results indicate that the FZ has a higher values than the HAZ and BM. The micro-hardness gradually decreases in the HAZ from the FZ to the BM value. In other words, the micro-hardness in the HAZ is even higher than that in BM. The average micro-hardness in the Inconel 625 WM is 212 HV and slightly decreases to 185 HV in the BM. A gradual increase of the micro-hardness profile from BM to FZ was observed in the welds.

Fig. 4 shows the tensile stress versus strain curves of the Incoloy 800H WM. For comparison, tensile data of the as-received Incoloy 800H BM is also included. The tensile curve of the Incoloy 800H weld is located above that of as-received BM, prior to reaching the ultimate tensile strength. Upon closer examination, the weld shows a distinctly higher linear elastic stress or elastic limits and yield stress than that of the Incoloy 800H BM, while their ultimate tensile strengths (UTS) are similar. The increases in elastic limit and yield stress are expected to contribute to the enhancement of creep properties. Table 2 summarizes the mechanical properties of Incoloy 800H BM and its weld. Fig. 5(a) compares the yield stress at 0.2% residual strain and ultimate tensile strength (UTS) between the BM and the welds. The welds with Inconel 625 filler materials exhibited a high yield stress of 203 MPa, an increase of 72% compared to the BM (118 MPa), while the UTS only increased 5% from 224 MPa of BM to 236 MPa of WM. Fig. 5(b) compares the ductility of the Incoloy 800H BM and WM. The total plastic elongation of the BM is higher than the welded specimens. A closer examination showed that both Incoloy 800H BM and weld displayed relatively small uniform plastic deformation, but much larger non-uniform plastic deformation (Fig. 4). It is worth noting that both the BM and weld demonstrate a very high reduction in area (Table 2 and Fig. 5(b)) of more than 50%.

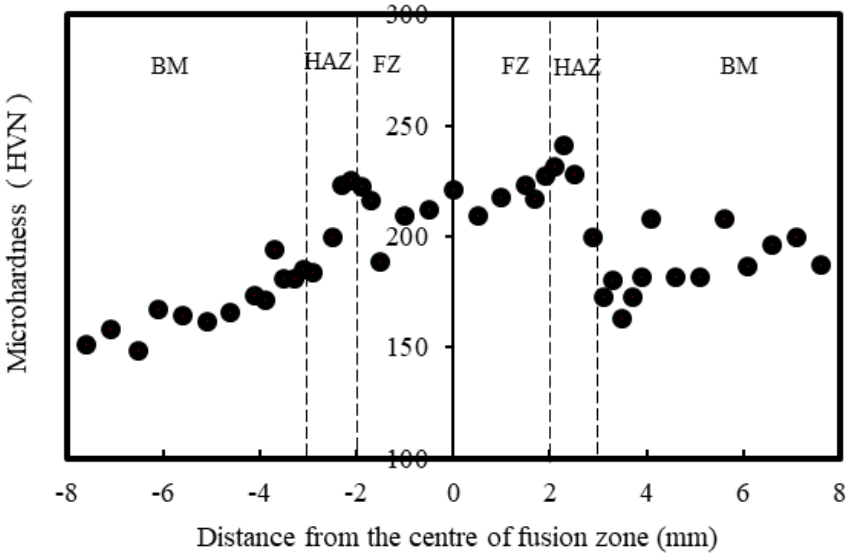

Figure 3: Effect of Filler Materials on Micro-Hardness Profile across Incoloy 800H Welds

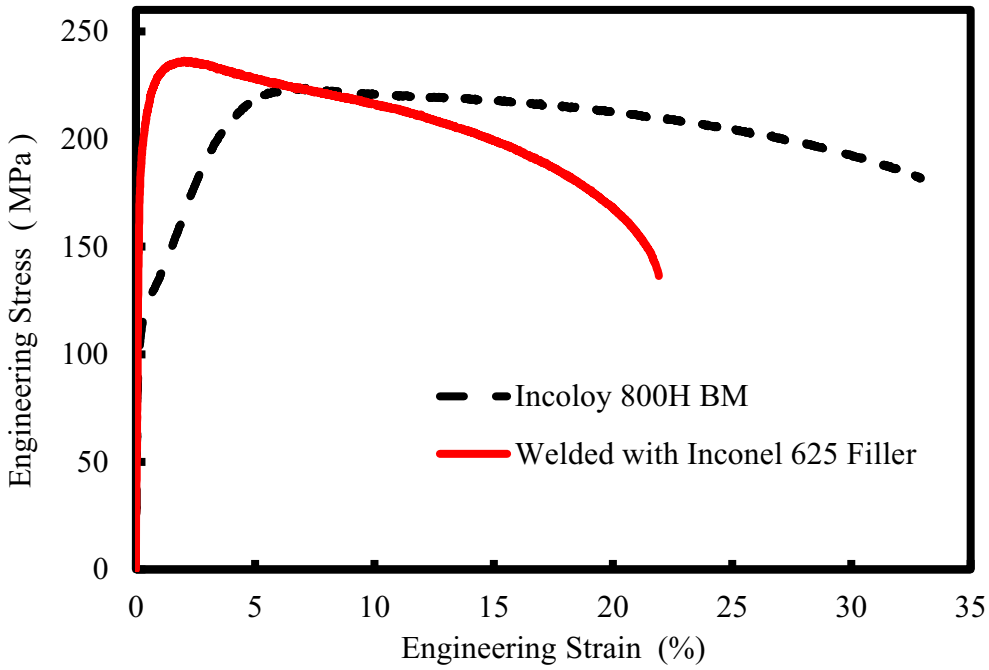

Figure 4: Comparison of Tensile Curves of Incoloy 800H BM and Weld

Table 2: Tensile Properties of Incoloy 800H and Its Weldments at 760 °C

BM & Weld	Yield Stress (MPa)	UTS (MPa)	Reduction in Area (%)	Plastic Elongation (%)
Incoloy 800H BM	118	224	64	26
Weld with Inconel 625 WM	203	236	54	15

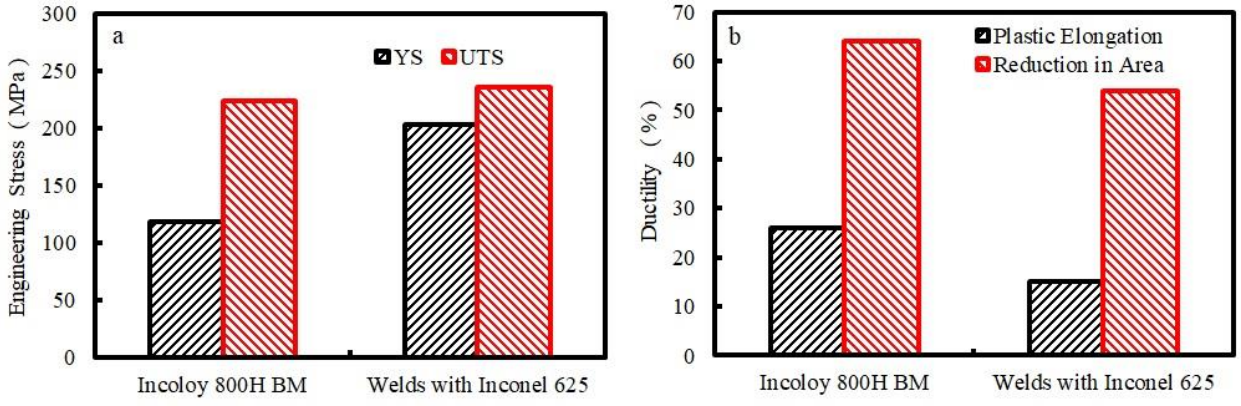

Figure 5: Comparison of Strength between Incoloy 800H BM and Welds with Inconel 625 Filler Material, (a) Strength, (b) Ductility.

3.3 Fracture Mode in Incoloy 800H BM and Weld

Fig. 6 shows the fracture mode of the Incoloy 800H weld. A micro-void accumulation fracture mode was displayed. The fracture surface shows obvious necking. Further examination showed that the Incoloy 800H weld fractured outside the welding zone while the full weld zones remained intact, as indicated by arrows in Fig. 6. This indicated that the strength of the welds was stronger than the BM at 760 °C.

Figure 6: Typical Fracture Mode of Incoloy 800H Welds with Inconel 625 Filler Material

3.4 Alloying Element Re-Distribution/Diffusion Produced by Welding in the Vicinity of Fusion Boundaries

The variation in major alloying elements (Fe, Ni, Cr, Nb, Mo, Mn, and Ti) across the fusion boundaries between Incoloy 800H BM and Inconel 625 WM within a 200 μm distance from the fusion boundary at both sides of the fusion line were examined by EDS, as shown in Fig. 7. Ni and Fe concentrations in Incoloy 800H were 30.8 wt. % and 45.5 wt. %, respectively, and 57.0% and 3.5%, respectively in Inconel 625 in the as-received condition. Additional 3.15~4.15% Nb and 8.0~10.0% Mo are contained in the Inconel 625 than those in the Inconel 800H. The nominal composition gradient is steeper between the BM and WM in before welding/as-received condition. The differences in composition gradients produced the driving force of element diffusion across the fusion line. Obvious element diffusion took place in an approximate range of 170 μm. Some Fe in the Incoloy 800H BM diffused into the Inconel 625 WM, and Ni diffused from the Inconel 625 WM into the BM. Further examination showed that the element distribution gradually increased/decreased across the fusion boundary, with no element depletion zone observed.

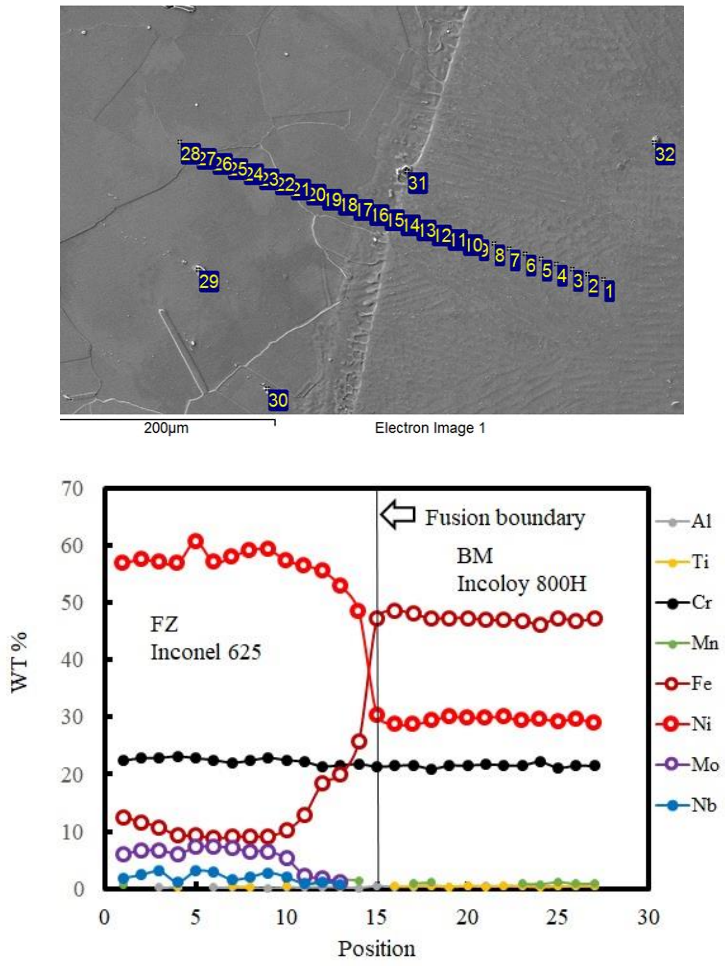

Figure 7: Distribution of Major Alloying Elements in the Vicinity of Fusion Boundaries of Incoloy 800H BM and Inconel 625 WM

3.5 TEM Characterization of Microstructure and Precipitates in Welds

The TEM characterization provides further insight into the strengthening mechanisms of the HAZ and FZ. Fig. 8 depicts the microstructure in the HAZ of Incoloy 800H alloys welded with Inconel 625 filler material. The HAZ shows Incoloy 800H with fine particles, with the fine particles identified as (Ti, Nb)(N, C) through EDS analysis. There are no large intermetallic particles, which would weaken the HAZ, and the fine particles would act to strengthen the material. The intermetallic compounds were not observed because of the formation of TiCN in the HAZ.

Fig. 9 shows the microstructure in the FZ. Small particles are observed, with EDS mapping indicating that they are (Ti, Nb)-rich carbo-nitride (Fig. 9(b) to (f)). As with the HAZ region, no large intermetallic particles are present, which would weaken the material, but instead the nano-sized precipitates are expected to contribute to increased strength in the Inconel 625 WM.

3.6 Strengthening Mechanisms in the HAZ and FZ

The weldability of Incoloy 800H and its resulting mechanical properties are largely dependent on their solidification behavior, which in turn depends on solute redistribution of alloying elements and the variation of grain size and morphology. The strengthening effects induced in the Incoloy 800H GTAW welds by the welding process include: solid solution strengthening due to re-melting of particles, second phase re-precipitation and re-distribution, grain size and microstructure refinements (equiaxed structure, columnar structure). A suitable filler material must be compatible with the properties of the BM. One major condition is that the filler material has to accept dilution from the BM without forming brittle intermetallic compounds or increasing susceptibility to cracking.

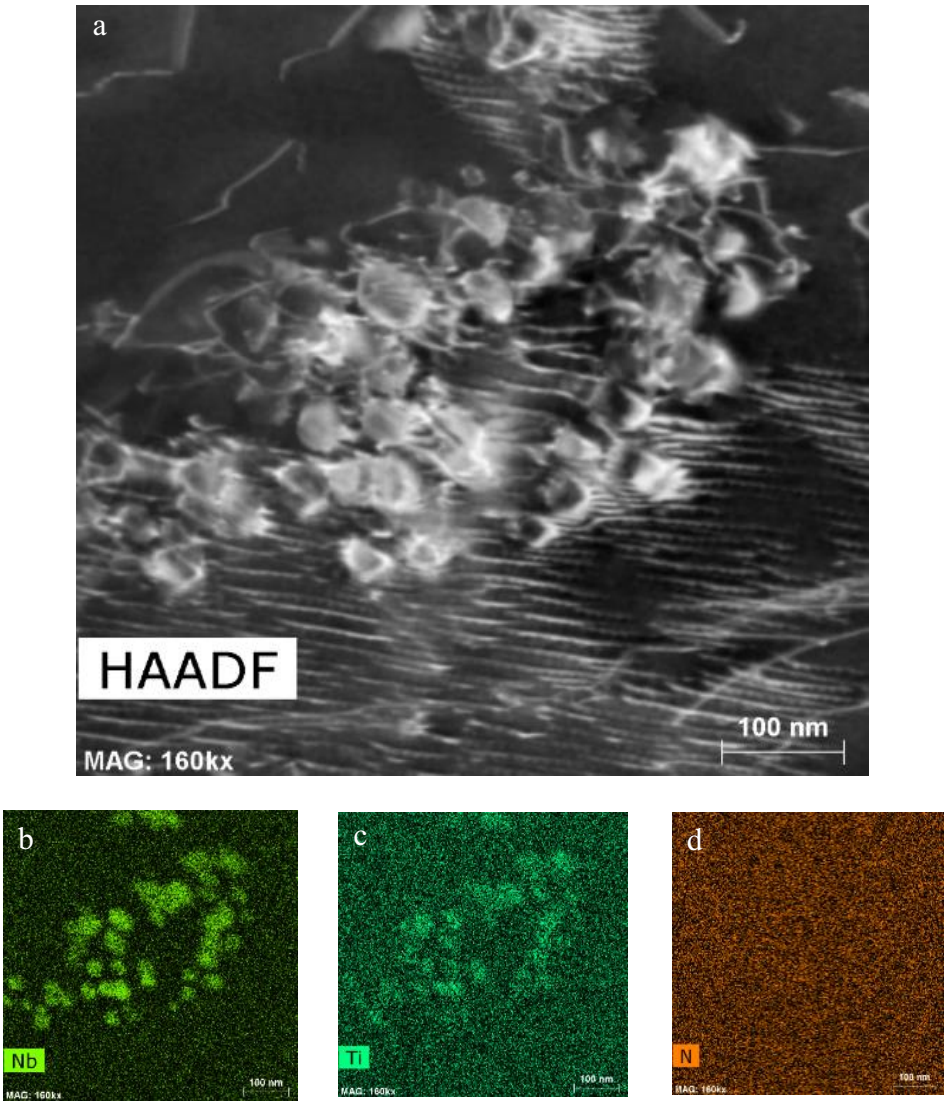

Figure 8: TEM Image (a) and ESD Mapping (b) to (c) of Incoloy 800H Welds with Inconel 625 Filler at the HAZ

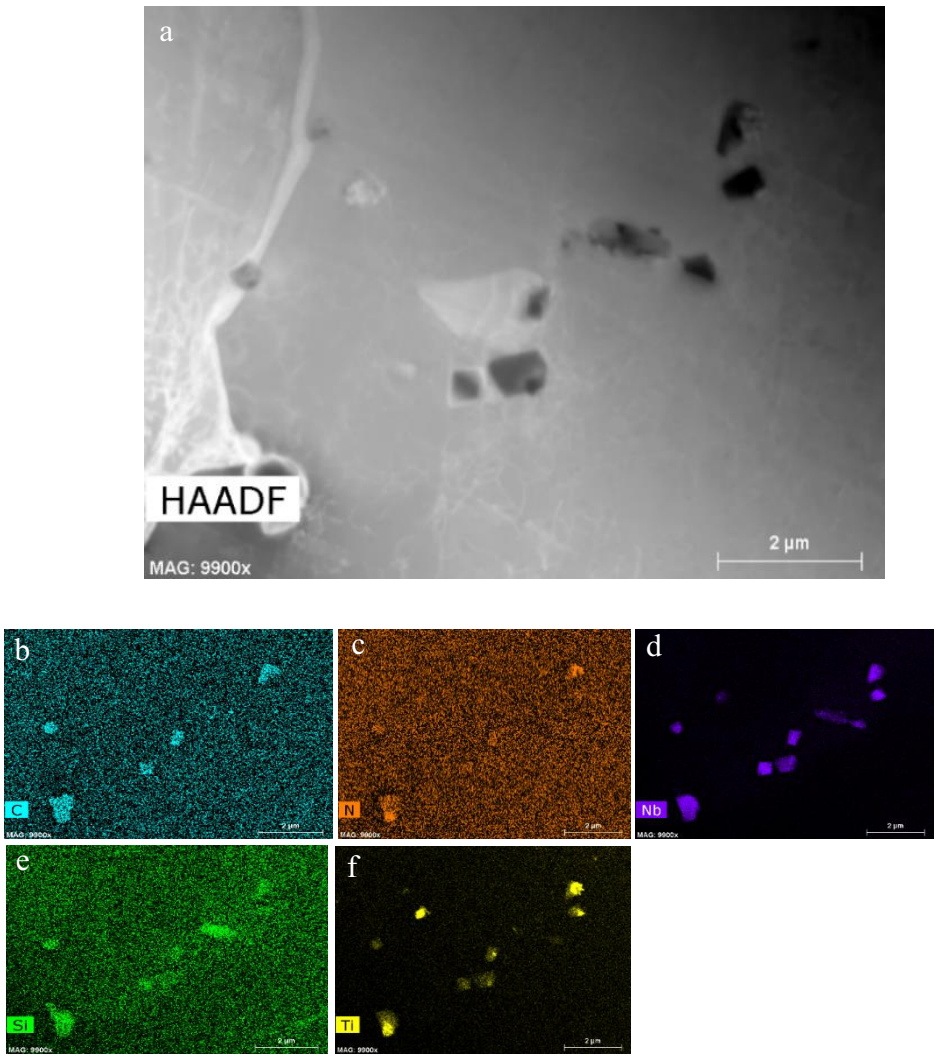

Figure 9: A Large Number of (Ti, Nb)(N, C) Particles Precipitated on Grain Boundary of Inconel 625 WM in the FZ, (a) TEM image, (b) to (g) Showing Mappings of Element Distributions

Both the BM (Incoloy 800H) and the WM (Inconel 625) are single phase austenitic alloys having a face-centered cubic (FCC) crystal structure. Their outstanding strength at high temperatures has widely been attributed to solid solution strengthening and the formation of secondary $M_{23}C_6$ carbides along grain boundaries [7-9]. Solid-solution strengthening is the predominant strengthening mechanism. The concentration of alloying elements contained in the BM and WM affect the degree of solid-solution strengthening and the solidification temperature range during welding. It also changes the extent and morphology of the secondary phases with the low melting point in welds.

The HAZ is an un-melted region of the BM where temperatures were high enough for solid-state transformations to occur: carbide dissolution or grain growth was therefore affected by the heating and cooling weld cycles. The welding process resulted in the re-melt of precipitates into matrix to increase the degree of solid solution strengthening. High concentrations of alloying in the WMs are beneficial to maintain high strength in the FZ (Fig. 3). Meanwhile, the high cooling

rate facilitates the nucleation but limits the growth of precipitates during welding. As a result, a large number of small precipitates were produced in the HAZ of the Incoloy 800H BM (Fig. 8). The precipitates significantly enhanced the yield strength of the Incoloy 800H weldments (Fig. 4, Table 2, and Fig. 5(a)). The welding process can also promote the dissolution of low-temperature stable phases in the HAZ and increase the solid solution strengthening mechanism, contributing to the enhancement of yield strength in welds [10].

4. Summary and Conclusions

In order to enhance tensile and creep properties of Inconel 800H welds at high temperatures as applied to HTGRs, Inconel 625 was selected as a filler metal to join Incoloy 800H. The experimental results demonstrated that the Inconel 625 filler has material properties that support its use in high-temperature applications.

(1) Incoloy 800H welded with Inconel 625 filler material showed superior high temperature tensile strength compared to the BM, observing that failure occurred in the BM away from the FZ and HAZ during high temperature tensile testing. The welds with Inconel 625 filler material exhibited higher yield stress (203 MPa), an increase of 72% compared to the BM (118 MPa).
(2) Tensile-tested welds exhibited micro-void accumulation type ductile fracture modes. The total plastic elongation of the BM is higher than the welds. Both Incoloy 800H BM and welds demonstrate a very-high reduction in area of more than 50%.
(3) The strengthening effects induced in Incoloy 800H GTAW welds by the welding process include: solid solution strengthening due to re-melting of particles, second phase re-precipitation and re-distribution, grain size and morphology refinements (equiaxed structure, columnar structure).
(4) Alloying element diffusion took place in the vicinity of fusion boundary between Inconel 800H and Inconel 625 filler metal. The outstanding strength of welds at high temperatures can be attributed to solid solution strengthening and the formation of secondary-phase particles along grain boundaries.

Acknowledgements

The authors would like to thank Shane Audette, Dwayne Schultz, Robyn Sloan, and Gregory Kasprick for performing the welding and the tensile tests.

This study was funded by Atomic Energy of Canada Limited, under the auspices of the Federal Nuclear Science and Technology Program. The research was conducted at the Canadian Nuclear Laboratories.

5. References

[1] The Intergovernmental Panel on Climate Change (IPCC) special report on Global Warming of 1.5 °C, 2017.

[2] A Technology Roadmap for Generation IV Nuclear Energy Systems, GIF-002-00, U.S. DOE Nuclear Energy Research Advisory Committee and the Generation IV International Forum, December 2002.

[3] ASME Standard, an International Code: ASME Boiler and Pressure Vessel Code, Section III, Rules for Construction of Nuclear Facility Components, Division 5 High Temperature Reactors, 2019 July 1.

[4] Idaho National Laboratory Next Generation Nuclear Plant Project, NGNP High Temperature Materials White Paper, INL/EXT-09-17187, 2012 August.

[5] W. Ren, R. Swindeman, "Status of Alloy 800H in Considerations for the Gen IV Nuclear Energy Systems," Journal of Pressure Vessel Technology, Vol. 136, p. 054001, 2014.

[6] G. Kim, I.N.C. Kusuma, J.Y. Park, I. Sah, E.S. Kim, S.J. Kim, M.H. Kim, "Hot Tensile Behavior for Alloy 800H Base and Weld Metals," in the *Transactions of the Korean Nuclear Society Autumn Meeting,* Yeosu, Korea, 2018 October 25-26.

[7] E. El-Magd, G. Nicolini, M. Farag, "Effect of Carbide Precipitation on the Creep Behavior of Alloy 800HT in the Temperature Range 700°C to 900°C," Metallurgical and Materials Transactions A, Vol. 27A, pp. 747-756, 1996.

[8] R.N. Wright, Summary of Studies of Aging and Environmental Effects on Inconel 617 and Haynes 230, Idaho National Laboratory Idaho Falls, Idaho 83415, INL/EXT-06-11750, September 2006.

[9] W. Ren, T. Totemeier, M. Santella, R. Battiste, D.E. Clark, Status of Testing and Characterization of CMS Alloy 617 and Alloy 230, ORNL/TM-2006-547, August 31, 2006.

[10] R. Mouginot, H. Hänninen, Microstructures of nickel-base alloy dissimilar metal welds, Aalto University Research Report, Finland, 2013.